# Calorimetric and spectroscopic studies of the polymorphic phase behavior of a homologous series of n-saturated 1,2-diacyl phosphatidylethanolamines

Ruthven N. A. H. Lewis and Ronald N. McElhaney
Department of Biochemistry, University of Alberta, Edmonton, Alberta, Canada, T6G 2H7

ABSTRACT The polymorphic phase behavior of a homologous series of n-saturated 1,2-diacyl phosphatidylethanolamines was investigated by differential scanning calorimetry, $^{31}$P-nuclear magnetic resonance, and Fourier transform infrared spectroscopy. Upon heating, aqueous dispersions of dried samples of the short- and medium-chain homologues ($n \leq 17$) exhibit single, highly energetic transitions from a dry, crystalline form to the fully hydrated, liquid-crystalline bilayer at temperatures higher than the lamellar gel–liquid-crystalline phase transition exhibited by fully hydrated samples. In contrast, the longer chain homologues ($n \geq 18$) first exhibit a transition from a dehydrated solid form to the hydrated $L_\beta$ gel phase followed by the gel–liquid-crystalline phase transition normally observed with fully hydrated samples. The fully hydrated, aqueous dispersions of these lipids all exhibit reversible, fairly energetic gel–liquid-crystalline transitions at temperatures that are significantly higher than those of the corresponding phosphatidylcholines. In addition, at still higher temperatures, the longer chain members of this series ($n \geq 16$) exhibit weakly energetic transitions from the lamellar phase to an inverted nonlamellar phase. Upon appropriate incubation at low temperatures, aqueous dispersions of the shorter chain members of this homologous series ($n \leq 16$) form a highly ordered crystal-like phase that, upon heating, converts directly to the liquid-crystalline phase at the same temperature as do the aqueous dispersions of the dried lipid. The spectroscopic data indicate that unlike the n-saturated diacyl phosphatidylcholines, the stable crystal-like phases of this series of phosphatidylethanolamines describe an isostructural series in which the hydrocarbon chains are packed in an orthorhombic subcell and the headgroup and polar/apolar interfacial regions of the bilayer are effectively immobilized and substantially dehydrated. Our results suggest that many of the differences between the properties of these phosphatidylethanolamine bilayers and their phosphatidylcholine counterparts can be rationalized on the basis of stronger intermolecular interactions in the headgroup and interfacial regions of the phosphatidylethanolamine bilayers. These are probably the result of differences in the hydration and hydrogen-bonding interactions involving the phosphorylethanolamine headgroup and moieties in the polar/apolar interfacial regions of phosphatidylethanolamine bilayers.

## INTRODUCTION

The diacyl phosphatidylethanolamines (PEs)[1] are important structural components of the cell membranes of many procaryotic and virtually all eucaryotic organisms. To date, a substantial amount of data on the physical properties of this class of membrane lipids has been accumulated (1–3), and from such studies it is expected that at low temperatures, fully hydrated dispersions of the 1,2-diacyl PEs form $L_\beta$ type of lamellar gel phases in which the all-*trans* acyl chains are essentially parallel to the bilayer normal. Upon heating, these lipids exhibit a fairly energetic and highly cooperative chain-melting transition (i.e., the gel–liquid-crystalline or $L_\beta/L_\alpha$ transition) at temperatures higher than those exhibited by phosphatidylcholines (PCs) of similar acyl chain composition. Moreover, unlike the common PCs, further heating of the liquid-crystalline phase of many PEs results in a weakly energetic, higher temperature transition in which the lamellar phase converts to an inverted nonlamellar structure. With most of the PEs studied so far, this transition corresponds to the conversion of the lamellar liquid-crystalline phase to an inverted hexagonal phase (i.e., a $L_\alpha/H_{II}$ transition), but under certain circumstances some PEs may exhibit direct transitions from the gel phase to the $H_{II}$ phase (4, 5), whereas with other PEs or under different experimental conditions, conversions from the lamellar phase to an inverted cubic phase can occur (5, 6). The fact that many PEs form inverted nonlamellar phases under physiologically relevant conditions of pH and hydration, coupled with the fact that the so-called "nonbilayer-forming" lipids comprise a sizable fraction of the lipids of all natural biomembranes (7–9), has provided the impetus for many studies targeted at both an understanding of the functional role of PEs (and other nonbilayer forming lipids) in cell membranes and at an understanding of underlying principles that predispose any class of lipids to form inverted nonlamellar phases (for reviews see references 10–13).

Despite considerable biological and biophysical interest in the PEs, there is yet to be the type of thorough characterization of their polymorphic phase behavior comparable with that performed on the diacyl PCs. At this time, such physical data are only available for a few even-chain, n-saturated 1,2-diacyl PEs (see reference 3 and others cited therein). From the available data, it is clear that in addition to the properties described above, aqueous dispersions of the shorter chain homologues of the n-saturated 1,2-diacyl PEs also form one or more condensed crystal-like ($L_c$) phases upon long-term incu-

Address correspondence to R. N. McElhaney.

[1] *Abbreviations used in this article:* DSC, differential scanning calorimetry; FT-IR, Fourier transform infrared; NMR, nuclear magnetic resonance; PC, phosphatidylcholine; PE, phosphatidylethanolamine.


0006-3495/93/04/1081/16 $2.00

bation at low temperatures (14–16), and these are believed to be highly ordered lamellar structures in which the headgroup and interfacial regions are, at the very least, substantially dehydrated (14, 17, 18). To date, this aspect of the polymorphic phase behavior of the shorter chain n-saturated diacyl PEs has been studied by techniques such as differential scanning calorimetry (DSC) (14, 15), dilatometry (16), x-ray diffraction (14), densitiometry (18), and quasielectric light scattering (19), and such studies indicate that the $L_c$ phases of these PEs are very stable structures that convert directly to the liquid-crystalline phase at temperatures well above those of the $L_\beta/L_\alpha$ phase transitions of the lipid concerned. However, such detailed investigations have been performed on only a few PEs. Furthermore, although there have been studies of the effect of variations in acyl chain length (20, 21), acyl chain structure (21), and the effect of other chemical modifications of the PE molecule (20), such studies have been performed mainly from the perspective of the sensitivity of the $L_\beta/L_\alpha$ phase transition and/or the lamellar/inverted nonlamellar phase transition to such chemical changes. Thus, whereas some aspects of the behavior of hydrated PE bilayers are reasonably well understood, there is still insufficient data to enable one to construct a complete picture of the effect of the various chemical modifications on the overall polymorphic phase properties of the PEs. Given the above, we have begun a study of the effects of variations in hydrocarbon chain length and structure on the polymorphic phase behavior of aqueous PE dispersions. Our approach is essentially similar to that which has been used previously in this laboratory for the study of PCs and glycolipids (see references 22–25 and others cited therein). We report here the results of our initial DSC, $^{31}$P-nuclear magnetic resonance (NMR), and Fourier transform infrared (FT-IR) spectroscopic studies of the polymorphic phase behavior of a homologous series of n-saturated 1,2-diacyl PEs.

## MATERIALS AND METHODS

The PEs used in this study were synthesized from their respective PCs by transphosphatidylation using cabbage phospholipase D (Sigma Chemical Co., St. Louis, MO) under the reaction conditions described by Comfurius and Zwaal (26). After a suitable time, the reaction was quenched by acidification to near pH 1 with cold hydrochloric acid and, after dilution with water, the mixture was extracted with chloroform. The chloroform layer was washed twice with water, dried by filtration through chloroform-wetted filter paper, and concentrated to dryness by rotary evaporation. The crude PE was then dissolved in chloroform and applied to a column of silicic acid (Biosil A; Bio-Rad Laboratories, Richmond, CA) in chloroform. The column was next washed with five column volumes of chloroform/methanol (95:5) and then developed with chloroform/methanol (75:25). The fractions containing PE were pooled, concentrated in vacuo, lyophylized from benzene, and stored at −20°C until required. Under our conditions we were unable to obtain reasonable yields 20:0 PE with the above procedure mainly because of the relatively low solubility of the 20:0 PC in the organic solvent mixture used for the transphosphatidylation. Thus, 20:0 PE was prepared by the hydrogenation of 1,2 di-*cis*-10 eicosenoyl PE that was itself prepared by the transphosphatidylation of the corresponding PC as described above. The precursor PCs were themselves synthesized from their respective fatty acids and purified by methods previously used in this laboratory (27, 28).

The methods used for preparing samples for DSC were as follows. In the case of the dried solid samples, 1–3 mg of the lyophylized sample were weighed into the Hastelloy capsules used with the DSC instrument (Hart Scientific, Pleasant Grove, UT), and 0.5 ml of water was added. After sealing the capsule, DSC thermograms were recorded with the Hart Scientific high-sensitivity differential scanning calorimeter operating at a scan rate of 15°C/h. To prepare the fully hydrated lipid samples, 3–4 mg of the dry sample were placed in a stainless steel large sample capsule (Perkin-Elmer Corp., Norwalk, CT) that was then warmed on a heated stage to a temperature in between the gel–liquid-crystalline phase transition temperature, $T_m$, and the lamellar/$H_{II}$ phase transition temperature $T_h$, of the given lipid. At this stage, 50 μl of distilled water was added, and the capsule was sealed and repeatedly heated and cooled at temperatures ranging from −5 to 100°C to ensure proper hydration. Afterward, DSC thermograms were recorded with a Perkin-Elmer DSC-2C differential scanning calorimeter equipped with a Perkin-Elmer 3700 Thermal Analysis data station. Once the initial DSC thermograms were recorded, the sample capsule was removed from the calorimeter and incubated under conditions appropriate for the formation of its highly ordered $L_c$ phase and then returned to the instrument for subsequent thermal analyses. The DSC data were analyzed using TADS software (Perkin-Elmer Corp.), software supplied by Hart Scientific, and other computer programs developed in this laboratory. At the end of all DSC analyses, the sample capsules were opened and their contents quantified using the gas chromatographic procedure previously used in this laboratory (27).

IR spectra were recorded for both dried and fully hydrated samples of these lipids. For the dried samples, diffuse reflectance spectra were recorded at room temperature using a diffuse reflectance accessory (Spectra-Tech, Inc., Stamford, CT). In the case of the fully hydrated samples, 3–4 mg of the dried lipid sample were mixed with 50 μl of $D_2O$ (or $H_2O$ as appropriate), and the mixture was heated and cooled as described above. The paste/dispersion obtained was then squeezed between two $BaF_2$ windows to form a 25-μm film, and the assembly was mounted in a heatable liquid cell. The cell was then placed in a sample holder that was heated and cooled by a computer-controlled water bath. With these samples, we found it more convenient to examine the normal gel–liquid-crystalline phase transition in the cooling mode since, with the shorter chain homologues, it enabled us to exert better control over the rate at which the $L_c$ phase forms at low temperature. The IR spectra were recorded with a FT-IR spectrometer (model FTS-40; Digilab Inc., Cambridge, MA) using the standard data acquisition methodology for these types of samples (29). The data acquired was processed using DDS software (Digilab Inc.) and other computer programs developed by the National Research Council of Canada. In cases where the spectra obtained consisted of broad overlapping bands, data processing usually involved the use of Fourier deconvolution to obtain fairly accurate estimates of the frequencies of the component bands, followed by curve-fitting procedures to obtain estimates of band width and intensity. Typically, band narrowing factors of 1.8–2.0 were used during deconvolution. Under our conditions, band narrowing factors of up to 2.5 could be used without introducing significant distortions to the spectra.

$^{31}$P-NMR spectra of the $L_\alpha$, $L_\beta$, and intermediate $L_c$ phases of these PEs were recorded with a high resolution spectrometer (model NT300-WB; Nicolet Instrument Corp., Madison, WI) operating at 121.47 MHz for the $^{31}$P nucleus. The spectra were obtained using single-pulse techniques and the data acquisition and data processing parameters described previously (30). $^{31}$P-NMR spectra of the $L_c$ phase were recorded with a solid-state spectrometer (model MSL 400; Bruker Instruments, Inc., Billerica, MA) operating at 161.98 MHz for $^{31}$P. Proton-decoupled spectra were recorded using a 5-μs pulse (90° flip angle), a

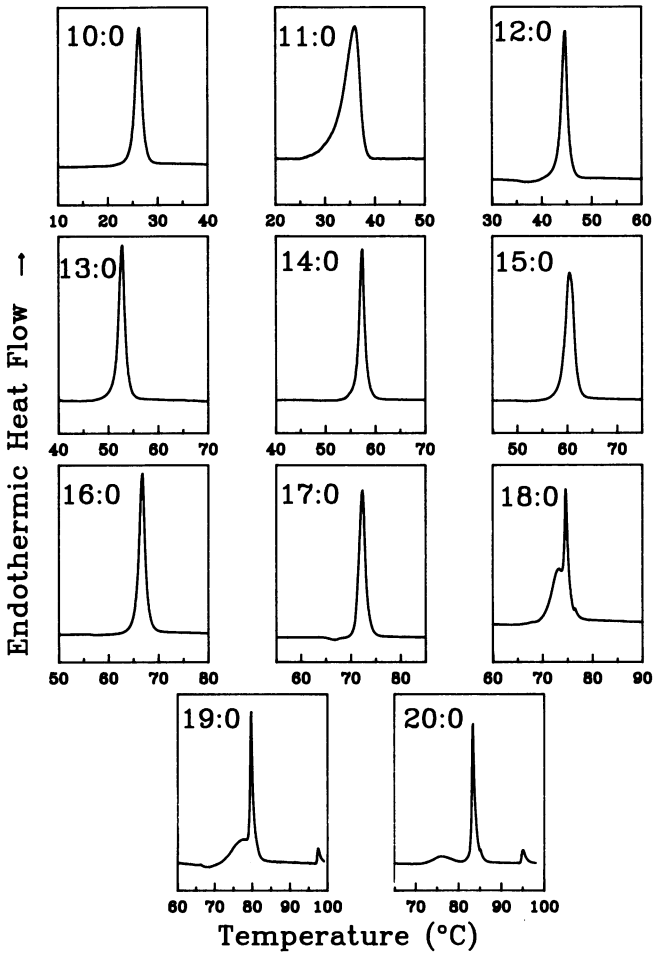


FIGURE 1 DSC heating thermograms observed on initial heating of aqueous dispersions of dried samples of the n-saturated diacyl PEs.

sweep width of ±125 kHz, and a recycle delay of 300 s. A 300-Hz line broadening function was used in the postprocessing of the free induction decay.

## RESULTS

## DSC

### Thermotropic phase behavior of aqueous dispersions of dried samples

Illustrated in Fig. 1 are the thermograms exhibited upon initial heating of aqueous dispersions of dried samples of the PEs studied. The short- and medium-chain compounds ($n$ = 10–17) all exhibit single, very energetic heating endotherms at temperatures above that of the typical gel–liquid-crystalline phase transition of the corresponding fully hydrated sample (see below). Moreover, the enthalpy changes characteristic of these processes (Table 1) are considerably greater than that commonly expected of simple chain-melting processes. This type of behavior has been observed in other studies of these PEs (31), and this thermotropic event has been ascribed to concurrent headgroup hydration, interfacial hydration, and chain-melting phenomena. With the longer chain compounds ($n$ = 18–20), our results suggest that the chain-melting and the polar/interfacial hydration phenomena are separated on the temperature scale, since two endothermic transitions are clearly resolved (Fig. 1). Of these, the lower temperature thermal event is probably attributable to the hydration phenomena, since it is fairly broad and is not observed on subsequent reheating of the sample. In contrast, the highly cooperative higher temperature event observed on initial heating of aqueous dispersion of these dried samples is still observed in subsequent reheatings of the sample and can therefore be assigned to the normal chain-melting phase transition of the fully hydrated lipid. We find that the thermodynamic properties of the highly cooperative chain-melting transition are indistinguishable from those of the typical gel–liquid-crystalline phase transition exhibited by fully hydrated samples of the same lipid (Tables 1 and 2). With the 19:0 and 20:0 compounds, we also observed additional weakly energetic transitions at temperatures above the chain-melting phase transitions. These events can be ascribed to the lamellar to inverted nonlamellar phase transitions of these lipids, since their thermodynamic properties are also indistinguishable from those exhibited by fully hydrated samples (Tables 1 and 2).

### Thermotropic phase behavior of fully hydrated samples

Heating and cooling thermograms of fully hydrated samples of the n-saturated diacyl PEs are shown in Fig. 2. From the thermograms shown therein and the numerical data listed in Table 2, it is clear that all of the lipids studied exhibit reversible transitions that are fairly energetic and highly cooperative. These transitions are attributable to the chain-melting phase transitions from their respective $L_\beta$ gel phases to the liquid-crystalline ($L_\alpha$) state. As expected, the transition temperatures and associated enthalpy changes increase progressively with increasing hydrocarbon chain length (Fig. 3 and Table 2). For many of the compounds studied, there was evidence for two or more exothermic peaks when the samples were cooled through the range of the gel–liquid-crystalline phase transition temperatures of the lipids concerned (Fig. 2). This behavior also has been reported in recent calorimetric and x-ray studies of 16:0 PE (32). Our spectroscopic studies indicate that the physical basis of all of the multiple cooling peaks were in fact similar and attributable to the "freezing" of the hydrocarbon chains into the all-*trans* conformation. We suspect that the multiple peaks probably arise from domain inhomogeneities that occur when the samples are heated to temperatures above $T_m$. In fact, from a visual inspection we find that hydrated samples of these PEs (particularly the

TABLE 1 **Thermotropic phase transitions exhibited by aqueous dispersions of dried samples of the n-saturated 1,2-diacyl phosphatidylethanolamines**

| | Transition temperature (°C) | | | | Transition enthalpy (kcal/mol) | | | |
|---|---|---|---|---|---|---|---|---|
| Sample | $L_c/L_\alpha$* | $L_c/L_\beta$* | $L_\beta/L_\alpha$ | $L_\alpha/H_{II}$ | $L_c/L_\alpha$* | $L_c/L_\beta$* | $L_\beta/L_\alpha$ | $L_\alpha/H_{II}$ |
| 10:0 | 26.2 | | | | 11.8 | | | |
| 11:0 | 36.0 | | | | 13.4 | | | |
| 12:0 | 44.7 | | | | 15.1 | | | |
| 13:0 | 52.8 | | | | 18.2 | | | |
| 14:0 | 57.4 | | | | 19.2 | | | |
| 15:0 | 60.5 | | | | 20.2 | | | |
| 16:0 | 66.0 | | | ND‡ | 22.3 | | | ND |
| 17:0 | 72.4 | | | ND | 24.7 | | | ND |
| 18:0 | | 73.3 | 74.2 | ND | | 9.5 | 10.6 | ND |
| 19:0 | | 77.9 | 79.2 | 97.5 | | 9.3 | 11.8 | 0.9 |
| 20:0 | | 75.7 | 83.4 | 94.3 | | 4.4 | 14.3 | 1.3 |

* The $L_c$ phase referenced here is the dried solid samples obtained by lyophylization from benzene. For the lipids with acyl chains ranging 10–17 carbon atoms, this refers to the type I solid that is spectroscopically similar to that obtained by the low-temperature annealing of fully hydrated samples. For the others, this refers to the type III solid form.

‡ Not determined. The $L_\alpha/H_{II}$ phase transitions of these dried samples were outside the range of the Hart Scientific instrument used to make the measurements.

longer chain samples) also tend to aggregate and adhere to the sides of the container when heated to temperatures well above $T_m$. This process is reversed upon cooling but oftimes displays some hysteresis. We therefore suggest that the multiple cooling exotherms observed are a reflection of such inhomogeneities and not the result of cooling irreversibility. Similar conclusions were deduced in recent calorimetric and x-ray studies (32). The longer chain members of this homologous series ($n \geq 16$) also exhibit an additional transition at temperatures above those of their respective $T_m$'s. This transition is the lamellar to $H_{II}$ phase transition (5, 20) and it is considerably less energetic than the gel–liquid-crystalline phase transition of the lipid (Table 2). As expected from previous studies (20, 21), this later transition is observed at progressively lower temperatures as the hydrocarbon chain length increases (Fig. 3 and Table 2).

TABLE 2 **Thermotropic phase transitions exhibited by fully hydrated aqueous dispersions of the n-saturated 1,2-diacyl phosphatidylethanolamines**

| | Transition temperature (°C) | | | Transition enthalpy (kcal/mol) | | |
|---|---|---|---|---|---|---|
| Sample | $L_c/L_\alpha$* | $L_\beta/L_\alpha$ | $L_\alpha/H_{II}$ | $L_c/L_\alpha$* | $L_\beta/L_\alpha$ | $L_\alpha/H_{II}$ |
| 10:0 | 26.2 | 2.0 | ‡ | 9.8 | 1.9 | ‡ |
| 11:0 | 36.0 | 16.9 | ‡ | 12.7 | 3.2 | ‡ |
| 12:0 | 44.7 | 31.3 | ‡ | 16.3 | 4.1 | ‡ |
| 13:0 | 52.8 | 42.1 | ‡ | 18.2 | 5.1 | ‡ |
| 14:0 | 57.4 | 50.4 | ‡ | 18.0 | 6.0 | ‡ |
| 15:0 | § | 58.4 | ‡ | § | 7.2 | ‡ |
| 16:0 | 66.0§ | 64.4 | 118.5 | § | 8.3 | 0.4 |
| 17:0 | § | 70.5 | 107.6 | § | 9.4 | 0.6 |
| 18:0 | § | 74.2 | 100.2 | § | 10.6 | 0.8 |
| 19:0 | § | 79.2 | 97.5 | § | 11.8 | 0.9 |
| 20:0 | § | 83.4 | 94.3 | § | 14.3 | 1.3 |

* The $L_c$ phases referenced here are those formed by low temperature annealing of fully hydrated samples.

‡ $L_\alpha/H_{II}$ transitions were not observed with these lipids. It is assumed that if these compounds do exhibit such transitions, they will occur at temperatures well above 125°C.

§ Under our experimental conditions, the $L_c$ phases of these lipids were not formed by low-temperature annealing of the DSC samples. Partial formation of the $L_c$ phase of 16:0 PE was observed with the FT-IR spectroscopic sample, and the transition temperature reported is an estimate obtained from the FT-IR experiment.

As also has been observed previously (14–16), prolonged low-temperature incubation of the fully hydrated samples of the shorter chain homologues results in the conversion of the $L_\beta$ gel phase to one or more highly ordered crystal-like $L_c$ phases. Furthermore, as reported previously for a number of PCs (27, 28) and various glycolipids (23, 24), we find that the formation of the $L_c$ phases of these compounds is a slow process that gets progressively more sluggish as the length of the fatty acyl chain increases. Thus, for example, the $L_c$ phase of 10:0 PE is completely formed by overnight incubation at temperatures near −10°C, whereas under the same conditions it takes 3–4 wk for complete formation of the $L_c$ phase of 14:0 PE, and with the very long chain PEs studied ($n \geq 17$) their $L_c$ phases were not formed over the timescale of this study (≅3 yr). As was also observed with the PCs and glycolipids, the rate of $L_c$ phase formation is considerably slower with the odd-numbered members of the homologous series. For example, we found it possible to induce the formation of the $L_c$ phase of 16:0 PE (albeit partially), but, despite the shorter chain length, we were unable to do the same with 15:0 PE. However, we also find that the formation of the $L_c$ phases of these compounds can be accelerated by a relatively brief (≅12 h) incubation at temperatures near −20°C, followed by the annealing of the sample at tem-

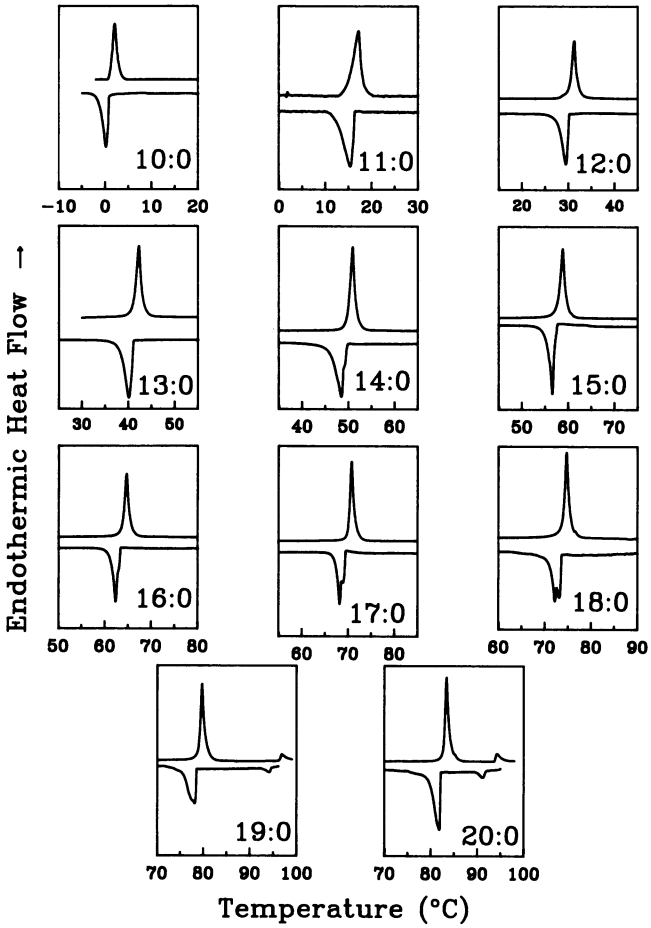


FIGURE 2 DSC heating and cooling thermograms of fully hydrated samples of the n-saturated diacyl PEs. The thermograms shown were all recorded at scan rates of $15°/h^{-1}$.

peratures some 1–5°C below the onset temperature of the $L_\beta/L_\alpha$ phase transition. Thus, with 14:0 PE, for example, complete conversion to its $L_c$ phase can be achieved by an overnight incubation at −20°C, followed by a 6-h incubation at 47°C, whereas the same process requires some 3–4 wk of isothermal incubation at temperatures near −5°C. Interestingly, our FT-IR spectroscopic studies (see below) indicate that incubation of the $L_\beta$ phase at temperatures near −20°C does not in itself induce the formation of the $L_c$ phase. Thus, with 14:0 PE we find that the FT-IR spectra recorded at the initiation and completion of the low-temperature incubation are indistinguishable from that of the $L_\beta$ phase. Moreover, after the low-temperature incubation, conversion to the $L_c$ phase proceeds at a reasonable rate only when the sample is heated to temperatures between 45 and 49°C. Thus, our results suggest that nucleation of the $L_c$ phase is accelerated by the short incubation at −20°C but that the growth of the $L_c$ phase is extremely sluggish at those temperatures. Thus, once nucleation is complete, the growth of the $L_c$ phase can then proceed fairly rapidly at higher temperatures. We also note that irrespective of the incubation procedures used, the IR spectroscopic and calorimetric "signatures" of the stable $L_c$ phases formed are identical. We thus conclude that the different incubation conditions used do not affect the structure of the $L_c$ phases that are formed. Thus, to save instrument time in our spectroscopic experiments, we routinely used the latter procedure to accelerate the formation of the $L_c$ phases of these compounds.

Despite the procedures used to accelerate the formation of the $L_c$ phase, conversion to this phase does not occur with all of the compounds studied. Under our conditions, complete conversion to the $L_c$ phase is observed only with the shorter chain PEs ($n$ = 10–14) and only a partial formation was observed with 16:0 PE. With the other PEs, we find no evidence for $L_c$ phase formation over the entire time course of this study (≅3 yr). However, once the $L_c$ phase forms, the thermotropic phase behavior of the sample is essentially indistinguishable from that of the dried sample described above. Thus, the transition endotherms are qualitatively similar to those shown in Fig. 1 (i.e., the $L_c$ phases decompose directly to the liquid-crystalline state at the same temperatures as did the aqueous dispersions of the dried samples). Moreover, the associated enthalpy changes (Table 2) are also considerably larger than those of the gel–liquid-crystalline phase transitions but tend to be slightly lower than those observed on initial heating of the dried samples (Tables 1 and 2). In these studies there is no calorimetric evidence for the formation of $L_c$-phase intermediates comparable with that previously reported for 12:0 PE (14). However, we believe that this may be the result of kinetic considerations because such intermediates were detected in our spectroscopic studies (see below).

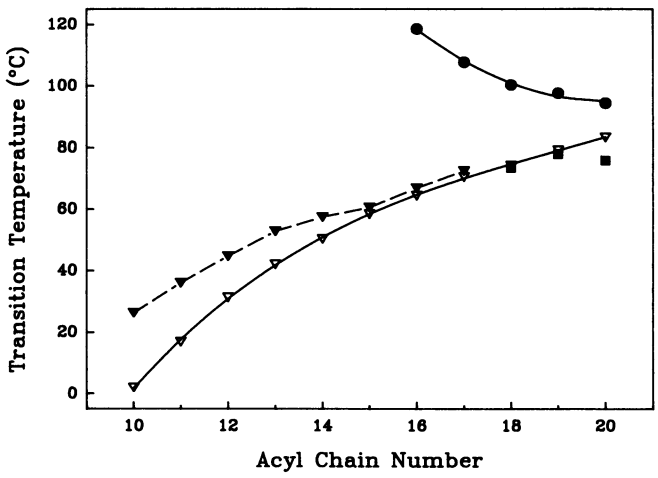


FIGURE 3 Chain-length dependence of the transition temperatures of the n-saturated diacyl PEs. The data shown illustrate the chain length dependence of (▽) $L_\beta/L_\alpha$ transition temperatures, (●) $L_\beta/H_{II}$ transition temperatures, (▼) $L_c/L_\alpha$ transition temperatures, and (■) $L_c/L_\beta$ transition temperatures.

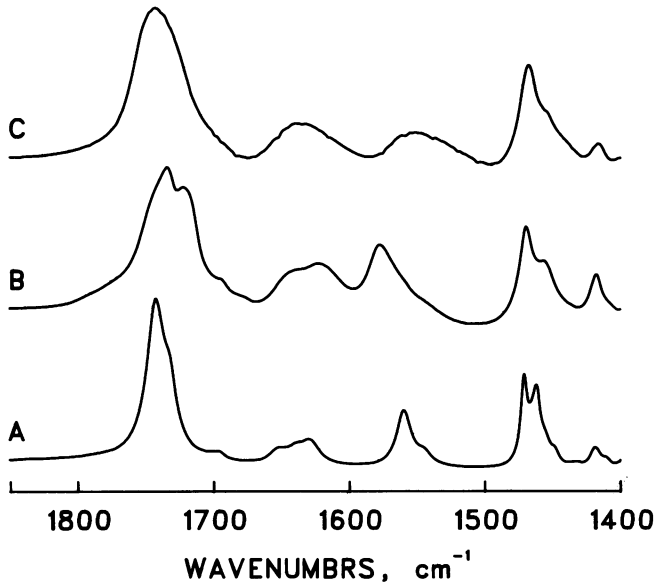


FIGURE 4 Diffuse reflectance FT-IR spectra of dry microcrystalline forms of the n-saturated diacyl PEs. The spectra shown represent the C=O stretching and $CH_2$ deformation regions of the infrared spectra of (*A*) the type I solid form, (*B*) the type II solid form, and (*C*) the type III solid form.

## FT-IR

### Studies of dried samples

Diffuse reflectance IR spectra of dried microcrystalline samples of the homologous series of PEs were recorded at room temperature. The data clearly suggest that three spectroscopically distinct types of microcrystalline solids can be formed. One of these (designated type I) appears to be a highly ordered crystalline form (judging from the very sharp bands in the IR spectrum; Fig. 4, spectrum *A*) and is only observed with samples of the short- and medium-chain members of the homologous series ($n$ = 10–17). The microcrystalline form that we have designated type II appears to be a more disordered type of solid (Fig. 4, spectrum *B*) and is only observed with samples of the shorter chain, even-numbered homologues ($n$ = 10, 12, and 14). This solid form appears to be unstable with respect to the more ordered type I, since it usually converts to that form on prolonged storage under our laboratory conditions. The other microcrystalline solid form, which we have designated type III, is observed with samples of all members of the homologous series. This form is usually observed soon after lyophylization of the sample from benzene, and the IR spectroscopic data are consistent with its being a considerably more disordered solid than either of the other solid forms observed, because the major absorption bands are considerably broader than those of the other solid forms (Fig. 4, spectrum *C*). With the short- and medium-chain homologues ($n < 18$), this form is apparently unstable and eventually converts to the more stable type I or type II form. However, with the long-chain homologues ($n$ = 18–20), the type III solid form appears to be more stable and is the predominant form that is observed. However, from our examinations of the IR spectra of the longer chain compounds, we sometimes find evidence for small populations of the other crystalline forms, particularly after these samples have been stored for extended periods of time. However, the populations of such forms are generally small and tend to decrease with increases in acyl chain length.

The IR spectra of the solid PE samples (data summarized in Table 3) also reveal many features that convey important structural information. The dominant feature of the spectrum of type III solid is that the absorption bands of moieties in both the polar headgroup and the polar/apolar interfacial region (e.g., the $_{\nu}PO_2^-$, $_{\delta}NH_3^+$, and $_{\nu}C{=}O$ bands) are very broad. This is consistent with the existence of an amorphous solid in which the lipid molecules may not have "crystallized" into any single structure, with the result that the environments around the vibrating groups in the headgroup and interfacial moieties are somewhat heterogenous. With the type I and type II solids, however, these bands are considerably sharper, and this is consistent with the existence of a more ordered type of solid in which there is, at the very least, the preponderance of a single crystalline form. For the type I solid form, it is also noteworthy that the IR absorption assigned to the asymmetric and symmetric $PO_2^-$ stretching vibrations appear predominantly as

**TABLE 3 Assigned bands of the IR spectra of dried samples of the n-saturated 1,2-diacyl phosphatidylethanolamines**

| | Frequency ($cm^{-1}$) | | |
|---|---|---|---|
| Vibrational mode | Solid type I | Solid type II | Solid type III |
| $_{\nu as}CH_3$ | 2,954 | 2,956 | 2,956 |
| $_{\nu as}CH_2$ | 2,924 | 2,924 | 2,925 |
| $_{\nu s}CH_2$ | 2,851 | 2,851 | 2,851 |
| $_{\delta}CCN^+$ and $_{\delta s}NH_3^+$ | 2,130 | 2,107 | 2,092 |
| $_{\nu}C{=}O$ | 1,742, 1,735 (sh) | 1,741, 1,734, 1,722 | 1,743 (broad) |
| $_{\delta as}NH_3^+$ | 1,651, 1,639 (sh) | 1,640, 1,623 | 1,634 (broad) |
| $_{\delta s}NH_3^+$ | 1,560 | 1,577 | 1,549 (broad) |
| $_{\delta}CH_2$ (main) | 1,471, 1,463 | 1,470 | 1,468 |
| $_{\delta as}CH_3$ | 1,456 | 1,456 | 1,456 |
| $_{\delta}CH_2$ ($\alpha$) | 1,419 | 1,418 | 1,416 |
| $_{\delta s}CH_3$ | 1,377 | 1,378 | 1,378 |
| $_{\nu as}PO_2^-$ | 1,224 | 1,261, 1,239, 1,222 | 1,239 (broad) |
| $_{\nu s}PO_2^-$ | 1,083 | 1,090 | 1,086 (broad) |
| $_{\nu as}CCN^+$ | 1,015, 1,001 | 1,021 | 1,034 |
| $_{\nu s}CCN^+$ | 917 | 912 | 911 |
| $_{\nu as}POC$ | 821 | 816 | 822 (broad) |
| $_{\nu s}POC$ | 761 | 761 | 753 (broad) |
| $_{\gamma}CH_2$ | 730, 719 | 719 | 721 |

$\nu$, stretching band; $\delta$, bending band; $\gamma$, rocking band; sh, shoulder; as, asymmetric; s, symmetric.

narrow bands near 1,224 and 1,083 $cm^{-1}$, respectively, and that the $NH_3^+$ bending bands are also very sharp. These observations are consistent with a structure in which the phosphate and amino bands are both immobilized. Moreover, the relatively low frequency of the phosphate bands (particularly the $_{vas}PO_2^-$ band) suggests that there is a strong hydrogen bond between the phosphate group and a hydrogen bonding donor group. In addition, the $CH_2$ scissoring and $CH_2$ rocking bands near 1,470 and 720 $cm^{-1}$, respectively, are both split into components of comparable intensity ($\cong$1,471 and 1,463 $cm^{-1}$ and 730 and 719 $cm^{-1}$, respectively). The above observations indicate that there is factor group splitting of the $CH_2$ scissoring and $CH_2$ rocking bands, which in turn indicates that in the type I solid form, the lipid hydrocarbon chains have "crystallized" into a structure in which their zigzag planes are perpendicular to each other. Also, in the C=O region of the spectrum, we note that the absorption band is very sharp and that it is centered near 1,742 $cm^{-1}$ with a small shoulder near 1,735 $cm^{-1}$. The sharpness of these absorption bands and the fact that they occur toward the higher end of the range expected of ester carbonyl groups suggest that the carbonyl groups are immobilized and that they are not hydrogen bonded to any hydrogen-bonding donor groups. For the type II solid form, however, we note that though the phosphate bands are sharper than observed with the type III solid, the absorption band contour is still smeared over a fairly broad range that includes both hydrogen-bonded and nonhydrogen-bonded forms. Thus, it is also possible that this solid form may be a mixture of heterogenous microcrystalline forms at least as far as the organization of the phosphate headgroup is concerned. Interestingly, the $CH_2$ scissoring and rocking bands each appear as single sharp bands near 1,470 and 719 $cm^{-1}$, respectively. These frequencies are toward the higher and lower ends of the range expected of main chain $CH_2$ scissoring and rocking bands, respectively, and suggest that the hydrocarbon chains have crystallized into a structure in which the zigzag planes are parallel to each other. Finally, we also note that in the type II solid form, the contours of the C=O stretching band contains a major sharp component near 1,722 $cm^{-1}$. This frequency of this component suggests that in this particular solid form there is a significant population of hydrogen-bonded ester carbonyl groups that are not present in the type I solid form.

### Hydrated samples: the gel–liquid-crystalline phase transition

The gel–liquid-crystalline phase transitions of these lipids were accompanied by distinct changes in the absorption bands arising from moieties in the hydrophobic and polar/apolar interfacial regions of these lipid bilayers. The absorption bands arising from the polar headgroups (e.g., the $PO_2^-$ stretching bands) exhibit no discernible changes at the gel–liquid-crystalline phase transition and will not be discussed here. Illustrated in Fig. 5 are the $CH_2$ stretching, the C=O stretching, and the $CH_2$ deformation regions of the IR spectra of hydrated 14:0 PE at temperatures just below and just above its gel–liquid-crystalline phase transition. The spectroscopic features shown typify the gel and liquid-crystalline phases of all members of this homologous series of lipids. In the $CH_3$ and $CH_2$ stretching region of the IR spectrum (between 2,800 and 3,000 $cm^{-1}$), these lipids exhibit distinctive bands with maxima near 2,850, 2,920, and 2,955 $cm^{-1}$. The $CH_2$ symmetric stretching band near 2,850 $cm^{-1}$ is of special significance because of its sensitivity to changes in the mobility and in the conformational disorder of the hydrocarbon chains (33). In the $L_\beta$ phase the $CH_2$ symmetric stretching band is relatively sharp and is observed near 2,849 $cm^{-1}$; on conversion to the $L_\alpha$ phase, this band broadens and its absorption maximum increases to frequencies near 2,851 $cm^{-1}$. The broadening of this band and frequency increases in the range 1.5–3 $cm^{-1}$ are diagnostic signatures of the chain-melting phase transitions of all the hydrated lipid bilayers studied so far (see references 34 and 35 and others cited therein). Such changes are the result of increased conformational disorder in the hydrocarbon chains and occur at the chain-melting phase transitions of all paraffinic compounds (33).

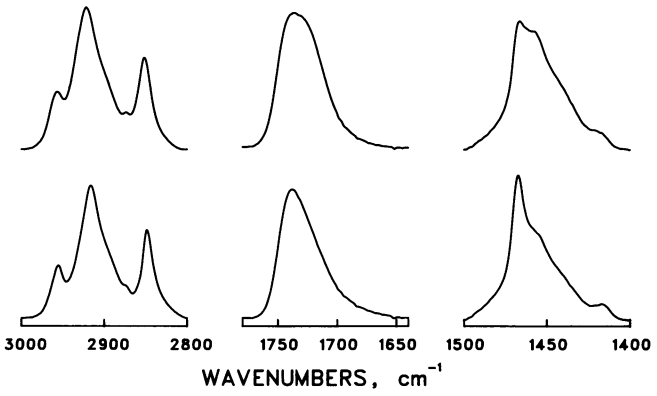


FIGURE 5 FT-IR spectra of the $L_\alpha$ (*top*) and $L_\beta$ (*bottom*) phases of fully hydrated samples of the n-saturated diacyl PEs. The spectra shown are presented in the absorbance mode and illustrate the band contours of regions near (*A*) the $CH_2$ symmetric stretching band, (*B*) the C=O stretching band, and (*C*) the $CH_2$ scissoring band.

Unlike the $CH_2$ stretching bands, which are sensitive to the conformation of the hydrocarbon chain, the $CH_2$ bending bands that occur near 1,468 $cm^{-1}$ are very sensitive to the lateral packing interactions of the hydrocarbon chains (36, 37). In the liquid-crystalline phase, these lipids all exhibit a very broad $CH_2$ scissoring band at 1,467 $cm^{-1}$, indicative of fairly mobile hydrocarbon chains with weak lateral interchain interactions (33). On conversion to the $L_\beta$ gel phase, the $CH_2$ scissoring band sharpens considerably (Fig. 5). The sharpening of the band upon freezing of the hydrocarbon chains is a

reflection of the marked reduction in the mobility of the hydrocarbon chains that occurs at liquid-crystalline to $L_\beta$ gel phase transition. We find that at temperatures just below the onset of the $L_\beta/L_\alpha$ chain-melting phase transition, the frequency of the $CH_2$ scissoring band is essentially similar to that of the $L_\alpha$ phase. This observation is consistent with a gel-phase organization in which the hydrocarbon chains are relatively loosely packed with relatively weak lateral interchain interactions (38, 39). However, we also find that on cooling of the $L_\beta$ phase to temperatures well below $T_m$, the $CH_2$ scissoring band broadens and eventually splits into two components with maxima near 1,472 and 1,466 $cm^{-1}$. This particular temperature-dependent change in the contours of the $CH_2$ scissoring band is a reflection of the strengthening of lateral interactions of the hydrocarbon chains once the reorientational fluctuations of the hydrocarbon chains are damped by cooling (36, 37). In this case the fact that the bands split into two components is also significant because it may be indicative of factor group splitting of the $CH_2$ scissoring band (36, 37). This in turn would suggest that in the $L_\beta$ phase of these PEs, the hydrocarbons chains may spontaneously assemble into a subcellular lattice with perpendicular hydrocarbon chains once chain reorientational fluctuations are damped (35, 36).

Several structurally interesting features were also apparent in the C=O stretching region of the IR spectra presented in Fig. 5. In the $L_\alpha$ phase the contours of the ester carbonyl band near 1,735 $cm^{-1}$ are fairly broad, and from its shape it is clear that it is a composite of two or more components. Using a combination of Fourier deconvolution and curve-fitting techniques, we find that the band contour is probably a composite of at least three components with maxima near 1,742, 1,728, and 1,714 $cm^{-1}$ (Fig. 5). Upon cooling to the $L_\beta$ phase, there is a marked decrease in relative spectral intensity in the low-frequency range of the band contour, and it would appear that this change in the contours of the C=O stretching band is the result of the "growth" of the high-frequency component ($\cong$1,742 $cm^{-1}$) at the expense of the two lower frequency bands (Fig. 5). These results are particularly significant since they are probably a reflection of changes in the hydrogen-bonding interactions in the polar/apolar interfacial region at the gel–liquid-crystalline phase transition of these PE bilayers. Moreover, these results also indicate that the contours of the C=O stretching bands of these hydrated PE bilayers differ significantly from those observed in studies of comparable PC bilayers (see comparison presented in Fig. 6). This is also a very significant observation since it is direct experimental evidence for differences between the hydrogen-bonding interactions in the polar/apolar interfacial regions of PC and PE bilayers. This and other aspects of the structural significance of these particular data will be explored further in the discussion.

### Hydrated samples: FT-IR spectroscopic characterization of the $L_c$ phase

Under our experimental conditions, 16:0 PE and the shorter chain lipids ($n$ = 10–14) were the only ones for which $L_c$ phases are formed when hydrated samples are annealed at low temperatures. For each of these lipids the formation of the $L_c$ phase is accompanied by major changes in several regions of the IR spectrum, and the $L_c$ phases that are eventually formed are spectroscopically indistinguishable from each other. As illustrated in Fig. 7, most of the absorption bands are very sharp, and this is consistent with the formation of a structure in which there has been a marked reduction in the mobility of most of the groups present in the lipid molecule. Interestingly, a comparison of the data shown in Figs. 4 and 7 indicates that the C=O stretching and the $CH_2$ scissoring regions of the IR spectra of the $L_c$ phase are virtually identical to that of the type I solid form described above. Indeed, we found that with the exception of differences attributable to the H/D exchange concomitant with the dispersal of the sample in $D_2O$ (e.g., the disappearance of the $_\delta NH_3^+$ bands), the observable regions of the IR spectra of the stable $L_c$ phase of these PEs are virtually identical to that of the type I solid described above. Thus, it would appear that the formation of the stable $L_c$ phase of these lipids is in fact a crystallization of these lipids comparable with that which occurs when the dried samples of the short- and medium-chain PEs ($n$ = 10–17) are prepared.

These IR spectroscopic studies also provide some evidence for the formation of $L_c$-like intermediate phases en route to the formation of the stable $L_c$ phase. In our FT-IR spectroscopic studies of the formation of the $L_c$ phases of the even-numbered, short-chain homologues ($n$ = 10, 12, and 14), we often obtain distinctive spectra comparable with that shown in Fig. 8. These spectra are clearly unlike those of the $L_\alpha$, $L_\beta$, or $L_c$ phases of these lipids and must be representative of a different structural form. Interestingly, the spectra shown in Fig. 8 appear to have many spectroscopic features that are similar to those of the type II solid described earlier (Fig. 4). Thus, this intermediate may be structurally similar to the type II solid form observed in these studies. Like the type II solid, this intermediate $L_c$ phase is also unstable with respect to a more stable form and is only observed with the even-numbered members of the homologous series.

## $^{31}$P-NMR spectroscopy

$^{31}$P-NMR spectra typical of the $L_\alpha$ and $L_\beta$ phases of aqueous dispersions of the n-saturated diacyl PEs are shown in Fig. 9. In both the $L_\beta$ and $L_\alpha$ phases, all of these lipids exhibit the axially symmetric powder patterns that are indicative of axially symmetric motion of the phosphodiester headgroup on the surface of a lipid bilayer (40, 41). As is typical of most phospholipid bilayers, the powder pattern exhibited by the gel phase is fairly broad

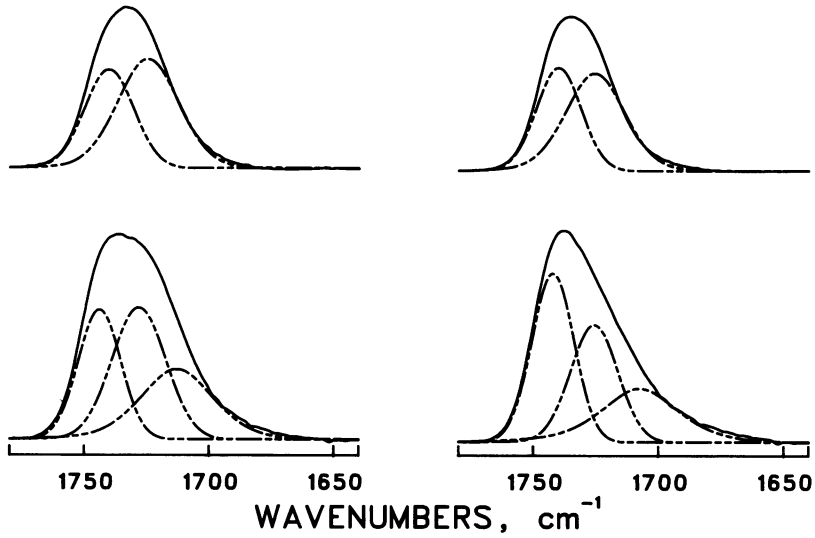


FIGURE 6 A comparison of the C=O stretching regions of the IR spectra of the $L_\alpha$ (*left*) and $L_\beta$ (*right*) phases of fully hydrated samples of 14:0 PC (*top*) and 14:0 PE (*bottom*). The spectra are shown in the absorbance mode with the solid lines representing the contours of the spectra actually acquired and the dashed lines representing our estimates of the position and relative intensities of the component bands.

(basal line width ≅ 90 ppm), indicating that the mobilities of the phosphate headgroups are in the slow range of axially symmetric motions that are feasible in a lipid bilayer. Upon melting of the hydrocarbon chains, there is an abrupt decrease in the width of the powder pattern observed with the result that the spectrum exhibited by the liquid-crystalline phase has a basal line width near 60 ppm. The latter indicates that in the liquid-crystalline phase the mobilities of the phosphate headgroups are in the fast range of axially symmetric motions that occur in a lipid bilayer. Fig. 9 also shows a $^{31}$P-NMR powder pattern obtained with a sample of 10:0 PE en route to the formation of its $L_c$ phase. Although the spectrum shown contains some of the characteristics of the axially symmetric powder pattern characteristic of its $L_\beta$ phase, it is evidently dominated by a very broad powder pattern (basal linewidth ≅ 230 ppm), the width of which is that expected for the so-called rigid limit powder pattern that has been observed with solid phospholipids (40, 41). The spectrum C shown is clearly that of a mixture of the $L_\alpha$ and $L_c$ phases. It should be noted that the broad powder pattern observed is probably that of an intermediate $L_c$ phase since it does not arise from the stable $L_c$ phase of this lipid. In fact, once the samples were incu-

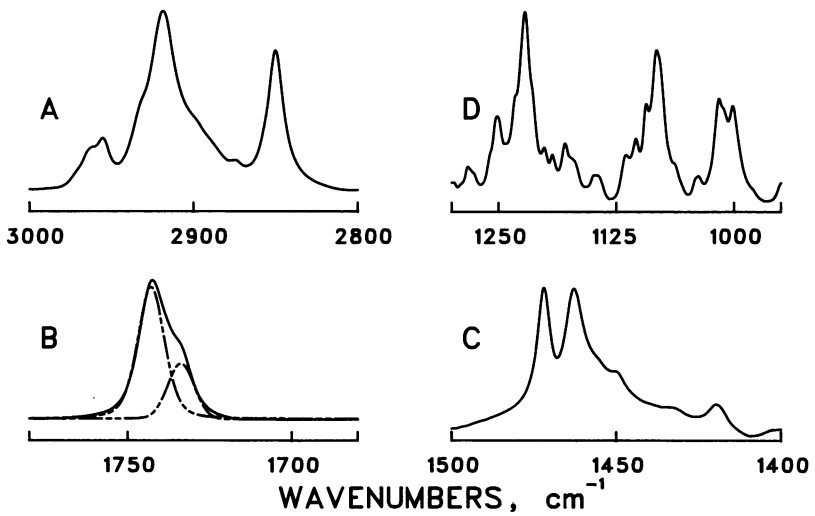


FIGURE 7 The $CH_2$ stretching (*A*), C=O stretching (*B*), $CH_2$ deformation (*C*), and $PO_2^-$ stretching (*D*) regions of the IR spectra of the stable $L_c$ phase of 12:0 PE. The spectra are shown in the absorbance mode. Where shown, the dashed lines represent our estimates of the position and relative intensities of the component bands.

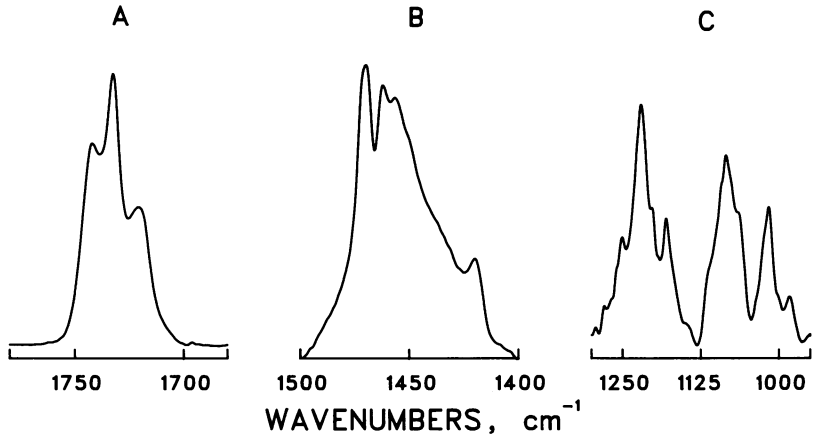


FIGURE 8 The C=O stretching (*A*), $CH_2$ deformation (*B*), and $PO_2^-$ stretching (*C*) regions of the IR spectrum of an intermediate $L_c$ phase of 14:0 PE. The spectra shown are presented in the absorbance mode and were acquired en route to the formation of the stable $L_c$ phase of the lipid.

bated under conditions conducive to complete conversion to the $L_c$ phase, their $^{31}$P-NMR spectra could not be recorded with the high resolution instrument despite the use of large sample sizes (≅100 mg) and the acquisition of a large number of transients (>100,000). Other workers have reported similar problems in their attempts at acquiring $^{31}$P-NMR spectra of the $L_c$ phase of 11:0 PE (42). We suspected that problems encountered by us and others (42) were a reflection of drastic changes in the relaxation properties of the $^{31}$P nuclei since the immobilization of phosphate groups can result in dramatic decreases in the spin lattice relaxation rates, $T_1$, of the $^{31}$P nucleus (43). In principle, the formation of an $L_c$ phase in which $^{31}$P nuclei have very long characteristic $T_1$'s can satisfactorily explain our difficulties in recording its spectrum. This is because long $T_1$'s will invariably necessitate the use of even longer recycle delays (minimum $T_1 \times 5$) that, for samples with very long $T_1$'s, may be so long that data acquisition becomes impractical. On account of these considerations and the FT-IR spectroscopic evidence that the stable $L_c$ phase is probably similar to that of a type I solid (see above), it seemed unlikely that we could successfully record its spectrum using high resolution instrumentation, and further attempts at obtaining the data were performed with a solid-state instrument.

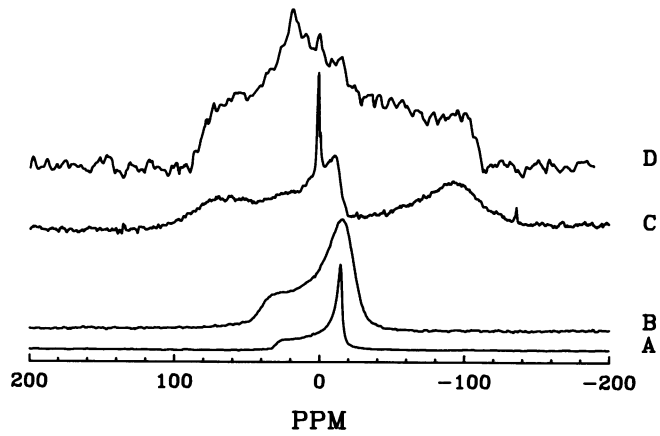


FIGURE 9 Proton-decoupled $^{31}$P-NMR powder patterns of hydrated PE samples. The powder patterns shown are (*A*) the $L_\alpha$ phase of ($T$ = 10°C), (*B*) the $L_\beta$ phase of 10:0 PE ($T$ = −2°C), (*C*) an intermediate $L_c$ phase of didecanoyl PE ($T$ = 0°C), and (*D*) the stable $L_c$ phase of 12:0 PE ($T$ = 24°C). The spectra *A*, *B*, and *C* were recorded with the high resolution instrument, and spectrum *D* was recorded with the solid-state instrument.

The solid-state NMR experiments were performed with the stable $L_c$ phase of 12:0 PE, and attempts were made to record spectra using both direct excitation and $^1$H-$^{31}$P cross-polarization techniques. In the direct excitation experiments we found that despite the higher transmitter power of the solid-state instrument, spectra with acceptable signal to noise ratios could be obtained only if the recycle delays are fairly long (≅300 s). $^{31}$P-NMR spectra of the $L_\alpha$, $L_\beta$ and intermediate $L_c$ phases could be adequately recorded with recycle delays of 2 seconds. This result confirms that the formation of the $L_c$ phase of these PEs is accompanied by dramatic decreases in the spin lattice relaxation rates of the $^{31}$P nuclei. As shown in Fig. 9, spectrum *D*, the spectrum obtained describes a so-called "rigid-limit" powder comparable with those observed in previous $^{31}$P-NMR spectroscopic studies of solid phospholipids (40, 41). This is consistent with the expectation that these lipids form a highly ordered $L_c$ phase in which the phosphate groups are essentially immobile on the $^{31}$P-NMR timescale. Since the long $T_1$'s of the $^{31}$P-nuclei will make data acquisition very expensive of instrument time, the feasibility of using $^1$H-$^{31}$P cross-polarization methods was also investigated. Such data acquisition methodology was expected to produce better results because, in addition to its higher intrinsic detection sensitivity, the practical limits to data acquisition will be determined by the proton relaxation rates that, under normal circum-

stances, tend to be considerably faster than those of $^{31}P$ nuclei. However, although we found it possible to record the $^{31}P$-NMR spectrum of the stable $L_c$ phase using $^{1}H$-$^{31}P$ cross-polarization methods (achieved with a 5-$\mu$s 90° pulse, a $^{1}H$-$^{31}P$ contact time of 20 ms, and a recycle delay of 30 s), the optimization of conditions for polarization transfer was extremely difficult because the proton spin lattice relaxation rates were themselves very slow. Thus, despite the theoretical benefits of the cross-polarization data acquisition methodology, it offered little practical advantage over the direct excitation methods. Nevertheless, the $^{1}H$-$^{31}P$ cross-polarization experiments clearly indicate that there is a dominant population of slowly relaxing protons in contact with the $^{31}P$ nucleus. This observation has significant structural implications that will be explored further in the discussion.

## DISCUSSION

These studies provide additional data pertinent to the physical basis of the polymorphic phase behavior of aqueous dispersions of the n-saturated 1,2-diacyl PEs and to the basis of the differences between these bilayers and the more intensively studied PC bilayers. These data provide the first complete set of thermodynamic measurements of the polymorphic phase behavior of n-saturated diacyl phosphatidylethanolamines of biologically relevant hydrocarbon chain lengths. From the data obtained, it is clear that the chain-length dependence of the thermodynamic data on the $L_\beta/L_\alpha$ and $L_\alpha/H_{II}$ phase transitions of fully hydrated samples of these PEs is relatively straightforward. Our thermodynamic measurements of the $L_\beta/L_\alpha$ phase transitions of these lipids are in general agreement with previously published studies of the even-numbered PEs (for data compilations see references 1–3) and 11:0 PE (42), and our new data on the other odd-numbered homologues and 10:0 PE are compatible with what would be predicted by interpolation or extrapolation from previously published work. Also, our measurements of the transition temperatures and enthalpy changes associated with that process follow the trends expected from previous studies (44). In the case of the $L_c/L_\alpha$ phase transitions of these lipids, however, there is also good agreement between the transition temperatures determined by us and others (see references 14–16, 31, 42, 45) but little agreement between our determinations of the transition enthalpy and other determinations previously reported (see references 14–16, 31, 42, 45). We find that there is considerable variability in the enthalpy values previously reported for the $L_c/L_\alpha$ phase transitions of these lipids (e.g., values for 14:0 PE range from 12 to 19 kcal/mol), and our values fall in the high end of the range of values reported so far. Given that PEs are known to form different crystalline structures when isolated from different solvents (17, 46) and the slow rates at which some samples convert to the $L_c$ phase, we suggest that the root causes of this variability are sample to sample variations in the microcrystalline structure of the various PEs studied and, possibly, variations in the extent of conversion to the $L_c$ phase.

From our spectroscopic data it is also clear that the stable $L_c$ phases of this homologous series of PEs describe an isostructural series. This is in marked contrast to the corresponding diacyl PCs for which the structure of the stable $L_c$ phases changes significantly with changes in acyl chain length (47, 48). The data also indicate that the stable $L_c$ phase is a highly ordered crystalline structure that is spectroscopically similar to one of the solid polymorphs (i.e., the type I solid) that forms under our laboratory conditions. When in aqueous dispersion, both the $L_c$ phase and the type I solid melt directly to the liquid-crystalline phase at temperatures above the gel–liquid-crystalline phase transitions of the hydrated sample. The data also indicate that the difference between the melting temperatures of the $L_c/L_\alpha$ (i.e., the transition temperatures of both the $L_c$ phase and the type I solid) and the $L_\beta/L_\alpha$ phase transitions decreases with increases in acyl chain length (Fig. 3). Indeed, an extrapolation of this trend suggests that for acyl chain lengths longer than 18 carbon atoms, the $L_c$ phases of these lipids should decompose to the $L_\beta$ phase at temperatures below the onset of the $L_\beta/L_\alpha$ phase transition. However, we were unable to test this hypothesis because the stable $L_c$ phases (or type I solid forms) of the longer chain lipids are not formed under our conditions.

Our studies of dried solid samples also provide some interesting and relevant data. We find that these PEs can adopt at least three spectroscopically distinct polymorphs. With PEs, such polymorphism is not unexpected, since it is well known that they can crystallize into different polymorphic forms and that the particular polymorph formed is strongly dependent on the solvent from which it was dried or crystallized (17, 46). Two of the polymorphic forms observed in these studies (i.e., type I and type II solids) appear to be spectroscopically similar to, though not identical with, the two 16:0 PE polymorphs reported in previous FT-IR spectroscopic studies (17), and the contours of the C=O stretching band of the type I solid seem to be similar to that reported for a substantially dehydrated sample of 16:0 PE (49). From our studies it would appear that the type I solid may be the most thermodynamically stable form since the other forms slowly convert to the type I solid on prolonged storage.

From the DSC studies of the dried samples, we also obtained data relevant to the energetics of hydration of these PE bilayers. In previous DSC studies of dried solid samples, the enthalpy difference between the $L_c/L_\alpha$ and $L_\beta/L_\alpha$ phase transitions (i.e., the energetic equivalent of a $L_c/L_\beta$ phase transition) was assigned to the heat of hydration of the headgroup and interfacial regions of the

lipid bilayer (31). However, we find that the magnitude of this difference increases with increases in acyl chain length. Moreover, the spectroscopic studies indicate that our dried samples ($n$ = 10–17) form an isostructural series of type I solid forms for which there is no evidence for any chain length–dependent differences in the structure and organization of the headgroup and polar/apolar interfacial regions of the solid. Given this, it is difficult to envisage how there can be any chain length–dependent variation of the observed enthalpy difference if headgroup and interfacial hydration are the sole contributors to the above observations. However, from our FT-IR spectroscopic data it is also clear that with the type I solid forms there is a strong factor splitting of both the $CH_2$ scissoring and $CH_2$ rocking bands, indicative of an organization in which there are strong lateral interactions between tightly packed perpendicular hydrocarbon chains. Furthermore, in the $L_\beta$ phase the hydrocarbon chains adopt a loosely packed organization in which the all-*trans* hydrocarbon chains are rotationally disordered with considerably weaker lateral interchain interactions. We therefore suggest that a significant fraction of the enthalpy change previously assigned to hydration phenomena must have arisen from rotational disordering of the hydrocarbon chains. To obtain rough estimates of the contributions of the chain packing and the hydration components to the total enthalpy change, the measured enthalpy difference was plotted as a function of the number of methylene segments (plot not shown). The incremental increase per $CH_2$ group can be estimated from the slope of the regression line and the hydration component estimated by extrapolation to zero carbon number. This analysis gives a hydration component of 3–4 kcal/mol of lipid and a chain-packing component increase of 750 calories/mol of lipid with each incremental increase of hydrocarbon length. Interestingly, with 20:0 PE (for which contamination of the type III crystalline form by the type I and type II forms is minimal), the enthalpy change associated with the conversion from the type III solid to the hydrated gel phase is 4.4 kcal/mol of lipid, a value that is close to the range expected from the crude estimates described above. That the enthalpy change measured for 20:0 PE should be close to that estimated for hydration phenomena alone seems very plausible because our FT-IR spectroscopic studies suggest that the type III solid form of this PE is a dehydrated (or a very poorly hydrated) solid in which there are rotationally disordered hydrocarbon chains with relatively weak lateral interchain interactions.

We also find that in both the $L_\alpha$ and $L_\beta$ phases the carbonyl ester interfacial regions of these PE bilayers are spectroscopically different from those of comparable PC bilayers. The contours of the C=O stretching band of these PEs are resolvable into at least three components with maxima near 1,742, 1,728, and 1,714 $cm^{-1}$. With hydrated PC bilayers, the C=O stretching band of their respective $L_\alpha$ and $L_\beta$ phases all seem to be composites of bands with maxima near 1,742 and 1,728 $cm^{-1}$ (Fig. 6). It was originally proposed that these component bands arise from conformational differences between the *sn*1 and *sn*2 ester carbonyl groups (40–52). However, recent studies using specifically labeled $^{13}C{=}O$ lipids show that each of these bands are themselves summations of comparable contributions from populations of *sn*1 and *sn*2 carbonyls (47, 53) and suggest that the bands near 1,728 and 1,742 $cm^{-1}$ probably arise from populations of hydrogen-bonded and nonhydrogen-bonded ester carbonyl groups, respectively (53). Thus, the additional low frequency band ($\cong$1,714 $cm^{-1}$) that we observe in the hydrated PE bilayers is indicative of another population of hydrogen-bonded ester carbonyl groups distinct from that present in hydrated PC bilayers. Although our observations suggest that there are two populations of hydrogen-bonded ester carbonyl groups, the identity of the donor groups to which they are bonded remains unknown. In PC bilayers, interfacial water molecules comprise the only source of donor groups that can hydrogen bond to the ester carbonyl groups. However, hydrated PE bilayers contain two possible sources of such hydrogen-bonding donors, interfacial water and the amine protons of the phosphorylethanolamine headgroup. Thus, it is possible that the two populations of hydrogen-bonded ester carbonyl groups present in PEs may arise from hydrogen bonding to interfacial water (probably the 1,728-$cm^{-1}$ band) and to the headgroup amine group (probably the 1,714-$cm^{-1}$ band). This possibility is supported by our studies of an *sn*2-$^{13}C{=}O$-labeled sample that indicate that the "low-frequency population" of ester carbonyl groups arises primarily from a subpopulation of *sn*2-carbonyl groups (Lewis, R. N. A. H., and R. N. McElhaney, unpublished data). This population gives rise to the C=O stretching band component near 1,714 $cm^{-1}$ and is not observed in either the $L_\beta$ or $L_\alpha$ phases of fully hydrated PC bilayers. Thus, if the above suppositions are true, then the fact that hydrogen-bonding interactions between the headgroup amine and the *sn*1 ester carbonyl groups are not observed can itself be rationalized by the conformational inequivalence between the *sn*1 and *sn*2 fatty acyl chains. From x-ray crystallographic studies of crystalline 1,2-diacyl phospholipids (54, 55) and from studies of hydrated bilayers of such lipids (56, 57), it is expected that the *sn*2 ester carbonyl group should be closer to the bilayer surface than is its *sn*1 counterpart. Thus, considering that the lipid bilayer restricts the mobility and conformation of the polar headgroup, it seems likely that when compared with the *sn*2 ester carbonyl groups, hydrogen-bonding interactions between the headgroup amine protons and the *sn*1 ester carbonyls may be considerably less probable, because the *sn*1 carbonyls would not be as accessible to the phosphoryl ethanolamine group as are their *sn*2 counterparts. However, irrespective of the identity of the

donor groups hydrogen bonded to the two populations of ester carbonyl groups, our results provide direct experimental evidence that PC and PE bilayers differ with respect to hydrogen-bonding interactions at the bilayer polar/apolar interfacial region. Although many of the physical differences between hydrated PC and PE bilayers are attributed to differences in the general nature of hydrogen-bonding interactions and to the capacity of the headgroup amine group of PE to hydrogen bond with other acceptor groups on the lipid molecule (see references 58–61 and others cited therein), to our knowledge there is little direct experimental support for such a premise.

The spectroscopic studies of both the solid samples and the stable $L_c$ phases of these PEs provide very useful insights into the nature of the driving forces behind the crystallization of these molecules. In general, our calorimetric and spectroscopic measurements are all compatible with the dehydrated crystalline structure that has been deduced from previous studies (14, 17, 18). We can conclude that these $L_c$ phases are very highly ordered crystal-like structures in which the hydrocarbon chains are tightly packed with perpendicular hydrocarbons (probably in an orthorhombic $\perp$ subcell) in which lateral interchain interactions are very strong. In addition, the ester carbonyl groups in the polar/apolar interfacial region of the bilayer are rigidly packed and are not hydrogen bonded to any donor groups. The frequencies of these two C=O bands were the same whether dispersed in $H_2O$ or $D_2O$ (data not shown). If these carbonyl groups were hydrogen bonded, then the frequencies observed in $H_2O$ dispersion would have been higher than that observed in $D_2O$. Interestingly, the frequencies of these ester carbonyl groups are themselves significantly lower than that expected of ester carbonyls in dry nonpolar solvents (62). Thus, despite the fact that the carbonyl groups are dehydrated, these groups evidently reside in a relatively polar environment. This observation suggests that there are close contact interactions between the polar groups in the interfacial region of the bilayer. In addition, in the $L_c$ phase the phosphorylethanolamine headgroups of these lipids must also be immobilized, because the $PO_2^-$ and C—N stretching bands are very sharp. Moreover, the frequency of the $PO_2^-$ stretching bands indicate that these phosphate groups are either hydrogen bonded or involved in a salt bridge with a polarizing cation. This, along with the evidence that the amine protons are themselves immobilized (note the sharpness of the $NH_3^+$ bending bands), suggests that the amine protons are probably "locked" in a long-lived hydrogen bond with the phosphate group. Similar conclusions have been deduced from single-crystal, x-ray diffraction studies of 12:0 PE (54). The suggestion that the phosphate groups are strongly immobilized in the $L_c$ phase also provides a rationale for our initial failure to obtain a $^{31}$P-NMR spectra of this phase, a problem also noted by others (42). Our results are consistent with the thesis that immobilization of the phosphate headgroup results in such drastic increases in the $T_1$'s of $^{31}$P nucleus (greater than several minutes; our estimates) that data acquisition using high resolution direct excitation NMR techniques becomes impractical. Interestingly, our solid-state $^1$H-$^{31}$P cross-polarization experiments also suggested that the dominant population of protons in contact with the $^{31}$P nucleii may themselves be strongly immobilized. This conclusion is also consistent with the suggestion that the headgroup amine protons are locked in a long-lived hydrogen bond (or a salt bridge) with the phosphate group. Interestingly, the problems that we have noted are not usually encountered in comparable $^{31}$P-NMR studies of the $L_c$ phases of hydrated PC bilayers (29, 30, 63, 64) or even dry microcrystalline powders of normal PCs (65, 66). Evidently, in the stable $L_c$ phase of these PEs the phosphate headgroups must be considerably less mobile than is the case with the majority of the PC bilayers which we have studied.

From our data it is also clear that the stable $L_c$ phases of this particular homologous series of lipids describe an isostructural series. (Under our conditions, the $L_c$ phase was only formed by 16:0 PE and all PEs with acyl chains ranging from 10 to 14 carbon atoms. Our data suggest that kinetic limitations precluded $L_c$ phase formation by the other PEs that were studied.) This is in marked contrast to many of the PCs that have been studied so far. With the PCs it is often the case that the gel-phase polymorphism exhibited by the homologues with odd-numbered fatty acyl chains is structurally and phenomenologically different from that exhibited by the homologues with even-numbered chains (27, 29, 63, 67–69). Interestingly, with the n-saturated diacyl PCs, there was no indication for any structural odd–even alternation in the types of $L_c$ phases formed, but the structure of the various stable $L_c$ phases varied markedly with acyl chain length (47, 48). Such chain length–dependent variations in the structure of the $L_c$ phases are probably ascribable to changes in the overall balance between the contributions of hydrophilic and hydrophobic forces to the overall free energy of stabilization of the various lipid bilayer phases (47). Thus, the fact that both shorter and longer homologues tend to form structurally similar $L_c$ phases suggests that for PEs the hydrophilic component to the overall free energy of stabilization of their $L_c$ phases dominates even when the acyl chains are fairly long. The finding that hydrophylic interactions in PE bilayers tend to be considerably stronger than those of PC bilayers may explain many of the differences in the physical properties of these two classes of phospholipids. Thus, the presence of strong polar interactions may account for the greater tendency of PE bilayers to crystallize into dehydrated solid forms when incubated at low temperatures. Moreover, such forces should also enhance the stability of all gel phases, resulting in higher melting transition temperatures. Finally, once the acyl chains are melted,

such strong intermolecular attraction in the polar and/or interfacial regions of PE bilayers should also decrease their radii of spontaneous monolayer curvature. The latter would constitute the basis of their greater propensity to form $H_{II}$ phases (70, 71).

We are indebted to Dr. Brian D. Sykes of the Department of Biochemistry at the University of Alberta for the generous availability of time on the Nicolet NMR spectrometer and to Drs. Frances Separovic and Bruce A. Cornell of the C.S.I.R.O. Food Research Laboratory (Sydney, Australia) for their contributions of personnel and instrument time toward the acquisition of solid-state $^{31}$P-NMR spectra of the $L_c$ phase of DLPE.

This work was supported by operating and major equipment grants from the Medical Research Council of Canada and by Major Equipment Grants from the Alberta Heritage Foundation for Medical Research.

*Received for publication 13 July 1992 and in final form 30 November 1992.*

## REFERENCES

1. Silvius, J. R. 1982. Thermotropic phase transitions of pure lipids and their modification by membrane proteins. *In* Lipid Protein Interactions. Vol. 2. P. C. Jost and O. H. Griffith, editors. John Wiley and Sons, New York. 239–281.
2. Small, D. M. 1986. Handbook of Lipid Research. Plenum Press, New York.
3. Marsh, D. 1990. Handbook of Lipid Bilayers. CRC Press, Inc., Boca Raton, FL.
4. Marsh, D., and J. M. Seddon. 1982. Gel to inverted hexagonal ($L_\beta$-$H_{II}$) phase transitions in phosphatidylethanolamines and fatty acid-phosphatidylcholine mixtures demonstrated by $^{31}$P-NMR spectroscopy and x-ray diffraction. *Biochim. Biophys. Acta.* 690:117–123.
5. Seddon, J. M., G. Cevc, R. D. Kaye, and D. Marsh. 1984. X-ray diffraction study of the polymorphism of hydrated diacyl and dialkylphosphatidylethanolamines. *Biochemistry.* 23:2634–2644.
6. Shyamsunder, E., S. M. Gruner, M. W. Tate, D. C. Turner, P. T. C. So, and C. P. S. Tilcock. 1988. Observation of inverted cubic phase in hydrated dioleoylphosphatidylethanolamine membranes. *Biochemistry.* 27:2332–2336.
7. Cullis, P. R., B. de Kruijff, M. J. Hope, A. J. Verkleij, R. Nayar, S. B. Farren, C. Tilcock, T. D. Madden, and M. B. Bally. 1983. Structural properties of lipids and their functional roles in biological membranes. *In* Membrane Fluidity in Biology. Vol. 1. R. C. Aloia, editor. Academic Press, New York. 39–81.
8. Rilfors, L., G. Lindblom, A. Wieslander, and A. Christiansson. 1984. Lipid bilayer stability in biological membranes. *Biomembranes.* 12:205–245.
9. Gruner, S. M., P. R. Cullis, M. J. Hope, and C. P. Tilcock. 1985. Lipid polymorphism: the molecular basis of non bilayer phases. *Annu. Rev. Biophys. Biophys. Chem.* 14:211–238.
10. Lindblom, G., and L. Rilfors. 1989. Cubic phases and isotropic structures formed by membrane lipids—possible biological significance. *Biochim. Biophys. Acta.* 988:221–256.
11. Seddon, J. M. 1990. Structure of the inverted hexagonal ($H_{II}$) phase, and non lamellar transition temperatures of phosphatidylethanolamines. *Biochim. Biophys. Acta.* 1031:1–69.
12. Seddon, J. M., J. L. Hogan, N. A. Warrender, and A. Pebay-Peyroula. 1990. Structural studies of phospholipid cubic phases. *Prog. Colloid & Polymer Sci.* 81:189–197.
13. Tate, M. W., E. F. Eikenbury, D. C. Turner, E. Shyamsunder, and S. M. Gruner. 1991. Nonbilayer phases of membrane lipids. *Chem. Phys. Lipids.* 57:147–164.
14. Seddon, J. M., K. Harlos, and D. Marsh. 1983. Metastability and polymorphism in the gel phase and fluid bilayer phases of dilauroylphosphatidylethanolamine. *J. Biol. Chem.* 258:3850–3854.
15. Chang, H., and R. M. Epand. 1983. The existence of a highly ordered phase of fully hydrated dilauroylphosphatidylethanolamine. *Biochim. Biophys. Acta.* 728:319–324.
16. Wilkinson, D. A., and J. F. Nagle. 1984. Metastability in the phase behavior of dimyristoyl phosphatidylethanolamine bilayers. *Biochemistry.* 23:1538–1541.
17. Mantsch, H. H., S. C. Hsi, K. W. Butler, and D. G. Cameron. 1983. Studies on the thermotropic behavior of aqueous phosphatidylethanolamines. *Biochim. Biophys. Acta.* 728:325–330.
18. Koynova, R., and H.-J. Hinz. 1990. Metastable behaviour of saturated phosphatidylethanolamines: a densitometric study. *Chem. Phys. Lipids.* 54:67–72.
19. Singer, M. A., L. Finegold, P. Rochon, and T. J. Racey. 1990. The formation of multilamellar vesicles from saturated phosphatidylcholines and phosphatidylethanolamines: morphology and quasi-electric lightscattering measurements. *Chem. Phys. Lipids.* 54:131–146.
20. Seddon, J. M., G. Cevc, and D. Marsh. 1983. Calorimetric studies of the gel-fluid ($L_\beta$-$L_\alpha$) and the lamellar inverted hexagonal ($L_\alpha$-$H_{II}$) phase transitions in dialkyl and diacylphosphatidylethanolamines. *Biochemistry.* 22:1280–1289.
21. Lewis, R. N. A. H., D. A. Mannock, R. N. McElhaney, D. C. Turner, and S. M. Gruner. 1989. The effect of fatty acyl chain length and structure on the lamellar gel to liquid-crystalline and lamellar to reversed hexagonal phase transitions of aqueous phosphatidylethanolamine dispersions. *Biochemistry.* 28:541–547.
22. Lewis, R. N. A. H., and R. N. McElhaney. 1992. The mesomorphic phase behavior of lipid bilayers. *In* Structure of Biological Membranes. P. L. Yeagle, editor. CRC Press, Boca Raton, FL. 73–155.
23. Mannock, D. A., R. N. A. H. Lewis, A. Sen, and R. N. McElhaney. 1988. The physical properties of glycosyl diacylglycerols. Calorimetric studies of a homologous series of 1,2-di-*O*-acyl-3-*O*-(β-D-glucopyranosyl)-*sn*-glycerols. *Biochemistry.* 27:6852–6859.
24. Mannock, D. A., R. N. A. H. Lewis, and R. N. McElhaney. 1990. The physical properties of glycosyl diacylglycerols. 1. Calorimetric studies of a homologous series of 1,2-di-*O*-acyl-3-*O*-(α-D-glucopyranosyl)-*sn*-glycerols. *Biochemistry.* 29:7790–7799.
25. Mannock, D. A., and R. N. McElhaney. 1992. Differential scanning calorimetry and x-ray diffraction studies of synthetic β-D-galactosyl diacylglycerols. *Biochem. Cell Biol.* 69:863–867.
26. Comfurius, P., and R. R. A. Zwaal. 1977. The enzymic synthesis of phosphatidylserine and purification by CM-cellulose column chromatography. *Biochim. Biophys. Acta.* 488:36–42.
27. Lewis, R. N. A. H., and R. N. McElhaney. 1985. Thermotropic phase behavior of model membranes composed of phosphatidylcholines containing isobranched phosphatidylcholines. 1. Differential scanning calorimetric studies. *Biochemistry.* 24:2431–2439.
28. Lewis, R. N. A. H., N. Mak, and R. N. McElhaney. 1987. Differential scanning calorimetric study of the thermotropic phase behavior of model membranes composed of phosphatidylcholines containing linear saturated fatty acyl chains. *Biochemistry.* 26:6118–6126.

29. Mantsch, H. H., C. Madec, R. N. A. H. Lewis, and R. N. McElhaney. 1985. Thermotropic phase behavior of model membranes composed of phosphatidylcholines containing isobranched fatty acids. 2. Infrared and $^{31}$P-NMR spectroscopic studies. *Biochemistry.* 24:2440–2446.

30. Lewis, R. N. A. H., B. D. Sykes, and R. N. McElhaney. 1988. Thermotropic phase behavior of model membranes composed of phosphatidylcholines containing *cis*-monounsaturated acyl chain homologues of oleic acid. Differential scanning calorimetric and $^{31}$P-NMR spectroscopic studies. *Biochemistry.* 27:880–887.

31. Chowdhry, B. Z., G. Lipka, A. W. Dalziel, and J. M. Sturtevant. 1984. Multicomponent phase transitions of diacylphosphatidyl ethanolamine dispersions. *Biophys. J.* 45:901–904.

32. Yao, H., I. Hatta, R. Koynova, and B. Tenchov. 1992. Time resolved x-ray diffraction and calorimetric studies at low scan rates. II. On the fine structure of the phase transition of hydrated dipalmitoyl phosphatidylethanolamine. *Biophys. J.* 61:683–693.

33. Mendelsohn, R., and H. H. Mantsch. 1986. Fourier transform infrared studies of lipid-protein interaction. *In* Progress in Lipid Protein Interactions. Vol. 2. A. Watts and J. J. H. H. M. De Pont, editors. Elsevier, New York. 103–146.

34. Snyder, R. G. 1967. Vibrational study of the chain conformation in the liquid n-paraffins and molten polyethylene. *J. Chem. Phys.* 47:1316–1360.

35. Mantsch, H. H., and R. N. McElhaney. 1991. Phospholipid phase transitions in model and biological membranes as studied by infrared spectroscopy. *Chem. Phys. Lipids.* 57:213–226.

36. Snyder, R. G. 1961. Vibrational Spectra of Crystalline n-Paraffins. Part II. Intermolecular Effects. *J. Mol. Spectrosc.* 7:116–144.

37. Snyder, R. G. 1979. Vibrational correlation splitting and chain packing for the crystalline alkanes. *J. Chem. Phys.* 71:3229–3235.

38. Casal, H. L., D. G. Cameron, and H. H. Mantsch. 1983. Infrared spectra of crystalline n-alkanes. Changes observed during the Phase I to Phase II transition. *Can. J. Chem.* 61:1736–1742.

39. Maroncelli, M., H. L. Strauss, and R. G. Snyder. 1985. The distribution of conformational disorder in the high temperature phases of the crystalline n-alkanes. *J. Chem. Phys.* 82:2811–2824.

40. Seelig, J. 1978. $^{31}$P Nuclear Magnetic Resonance and the headgroup structure of phospholipid membranes. *Biochim. Biophys. Acta.* 515:105–140.

41. Campbell, R. F., F. E. Meirovitch, and J. H. Freed. 1979. Slow motional line NMR lineshapes for very anisotropic rotational diffusion phosphorous-31 NMR of phospholipids. *J. Phys. Chem.* 83:525–533.

42. Xu, H., F. A. Stephenson, H. Lin, and C. Huang. 1988. Phase metastability and supercooled metastable state of diundecanoyl phosphatidylethanolamine bilayers. *Biochim. Biophys. Acta.* 943:63–75.

43. Withers, S. G., N. B. Madsen, and B. D. Sykes. 1985. $^{31}$P NMR relaxation studies of the activation of the coenzyme phosphate of glycogen phosphorylase. The role of motion of the bound phosphate. *Biophys. J.* 48:1019–1026.

44. Marsh, D. 1991. Analysis of chainlength dependence of lipid phase transition temperatures: main and pretransitions of phosphatidylcholines, main and non lamellar transitions temperatures of phosphatidylethanolamines. *Biochim. Biophys. Acta.* 1062:1–6.

45. Silvius, J. R., P. M. Brown, and T. J. O'Leary. 1986. Role of headgroup structure in the phase behavior of aminophospholipids. I. Hydrated and dehydrated lamellar phases of saturated phosphatidylethanolamine analogues. *Biochemistry.* 25:4249–4258.

46. Chapman, D., P. Bryne, and G. G. Shipley. 1966. The physical properties of phospholipids. I. Solid state and mesomorphic properties of some 2,3-diacyl-DL-phosphatidylethanolamines. *Proc. R. Soc. Lond.* A290:115–142.

47. Lewis, R. N. A. H., and R. N. McElhaney. 1990. The subgel phases of n-saturated diacyl phosphatidylcholines: A Fourier transform infrared spectroscopic study. *Biochemistry.* 29:7946–7953.

48. Lewis, R. N. A. H., and R. N. McElhaney. 1992. Structures of the subgel phases of n-saturated diacyl phosphatidylcholine bilayers: FT-IR spectroscopic studies of $^{13}C{=}O$ and $^{2}H$ labeled lipids. *Biophys. J.* 61:63–77.

49. Wong, P. T. T., and H. H. Mantsch. 1988. High pressure infrared spectroscopic evidence of water binding sites in 1,2 diacyl phospholipids. *Chem. Phys. Lipids.* 46:213–224.

50. Levin, I. W., E. Mushayakarara, and R. Bittman. 1982. Vibrational assignment of the sn-1 and sn-2 chain carbonyl stretching modes of membrane phospholipids. *J. Raman Spectrosc.* 13:231–234.

51. Mushayakarara, E., and I. W. Levin. 1982. Determination of acyl chain conformation at the lipid interface region. Raman spectroscopic study of the carbonyl stretching mode region of dipalmitoyl phosphatidylcholine and structurally related molecules. *J. Phys. Chem.* 86:2324–2327.

52. Mushayakarara, E., N. Albon, and I. W. Levin. 1982. Effect of water on the molecular structure of phosphatidylcholine hydrate. Raman spectroscopic analysis of the phosphate, carbonyl and carbon hydrogen stretching mode regions of 1,2 dipalmitoyl phosphatidylcholine dihydrate. *Biochim. Biophys. Acta.* 686: 153–159.

53. Blume, A., W. Hübner, and G. Messner. 1988. Fourier transform infrared spectroscopy of $^{13}C{=}O$ labeled phospholipids. Hydrogen bonding to carbonyl groups. *Biochemistry.* 27:8239–8249.

54. Hitchcock, P. B., R. Mason, K. M. Thomas, and G. G. Shipley. 1974. Structural chemistry of 1,2 dilauroyl-DL-phosphatidylethanolamine: molecular conformation and intermolecular packing of phospholipids. *Proc. Natl. Acad. Sci. USA.* 71:3036–3040.

55. Pearson, R. H., and I. Pascher. 1979. The molecular structure of lecithin dihydrate. *Nature (Lond.).* 281:499–501.

56. Hauser, H., I. Pascher, R. H. Pearson, and S. Sundell. 1981. Preferred conformation and molecular packing of phosphatidylethanolamine and phosphatidylcholine. *Biochim. Biophys. Acta.* 650:21–51.

57. Hauser, H., I. Pascher, and S. Sundell. 1988. Preferred conformation and dynamics of the glycerol backbone in phospholipids. An NMR and x-ray single crystal analysis. *Biochemistry.* 27:9166–9174.

58. Nagle, J. F. 1976. Theory of lipid monolayer and bilayer phase transitions: effect of headgroup interactions. *J. Membr. Biol.* 27:233–250.

59. Boggs, J. M. 1980. Intermolecular hydrogen bonding between lipids: influence on organization and function of lipids in membranes. *Can. J. Biochem.* 58:755–770.

60. Boggs, J. M. 1986. Effect of lipid structural modifications on their intermolecular hydrogen bonding interactions and membrane function. *Biochem. Cell Biol.* 64:50–57.

61. Boggs, J. M. 1987. Lipid intermolecular hydrogen bonding: influence on structural organization and membrane function. *Biochim. Biophys. Acta.* 906:353–404.

62. Mushayakarara, E. C., P. T. T. Wong, and H. H. Mantsch. 1986. Detection by high pressure infrared spectroscopy of hydrogen bonding between water and triacetylglycerol. *Biochem. Biophys. Res. Commun.* 134:140–145.

63. Lewis, R. N. A. H., and R. N. McElhaney. 1985. Thermotropic

phase behavior of model membranes composed of phosphatidylcholines containing ω-cyclohexyl fatty acids. Differential scanning calorimetric and $^{31}$P-NMR spectroscopic studies. *Biochemistry.* 24:4903–4911.

64. Lewis, R. N. A. H., H. H. Mantsch, and R. N. McElhaney. 1989. Thermotropic phase behavior of phosphatidylcholines with ω-tertiary butyl fatty acyl chains. *Biophys. J.* 56:183–193.
65. Kohler, S. J., and M. P. Klein. 1976. $^{31}$P nuclear magnetic resonance chemical shielding tensors of phosphorylethanolamine, lecithin and related compounds. Applications to headgroup motion in model membranes. *Biochemistry.* 15:967–973.
66. Rance, M., and R. A. Byrd. 1983. Obtaining high-fidelity spin ½ powder spectra in anisotropic media: phase cycled hahn echo spectroscopy. *J. Magn. Reson.* 52:221–240.
67. Mantsch, H. H., C. Madec, R. N. A. H. Lewis, and R. N. McElhaney. 1987. Thermotropic phase behavior of model membranes composed of phosphatidylcholines containing *dl*-methyl anteisobranched fatty acids. 2. An infrared spectroscopy study. *Biochemistry.* 26:4045–4049.
68. Mantsch, H. H., C. Madec, R. N. A. H. Lewis, and R. N. McElhaney. 1989. An infrared spectroscopic study of the thermotropic phase behavior of phosphatidylcholines containing ω-cyclohexyl fatty acyl chains. *Biochim. Biophys. Acta.* 980:42–49.
69. Church, S. E., D. J. Griffiths, R. N. A. H. Lewis, R. N. McElhaney, and H. H. Wickman. 1986. X-ray structure study of thermotropic phases in isoacylphosphatidylcholine multibilayers. *Biophys. J.* 49:597–605.
70. Kirk, G. L., S. M. Gruner, and D. L. Steim. 1984. A thermodynamic model of the lamellar to inverse hexagonal phase transition of lipid membrane-water systems. *Biochemistry.* 23:1093–1102.
71. Gruner, S. M. 1985. Intrinsic curvature hypothesis for biomembrane lipid composition: a role for non bilayer lipids. *Proc. Natl. Acad. Sci. USA.* 82:3665–3669.